A REVIEW OF HELIUM GAS TURBINE TECHNOLOGY FOR HIGH-TEMPERATURE GAS-COOLED REACTORS

HEE CHEON NO*, JI HWAN KIM and HYEUN MIN KIM
Department of Nuclear and Quantum Engineering,
Korea Advanced Institute of Science and Technology, Korea
*Corresponding author, E-mail : hcno@.kaist.ac.kr

Received January 26, 2007

Current high-temperature gas-cooled reactors (HTGRs) are based on a closed Brayton cycle with helium gas as the working fluid. Thermodynamic performance of the axial-flow helium gas turbines is of critical concern as it considerably affects the overall cycle efficiency. Helium gas turbines pose some design challenges compared to steam or air turbomachinery because of the physical properties of helium and the uniqueness of the operating conditions at high pressure with low pressure ratio. This report present a review of the helium Brayton cycle experiences in Germany and in Japan. The design and availability of helium gas turbines for HTGR are also presented in this study. We have developed a new throughflow calculation code to calculate the design-point performance of helium gas turbines. Use of the method has been illustrated by applying it to the GTHTR300 reference.

KEYWORDS : HTGR, Gas Turbines, Throughflow Analysis, Helium

1. INTRODUCTION

HTGRs were primarily developed in the United Kingdom, Germany and the United States of America commencing in the 1960s, and an advanced concept of a modular HTGR coupled to a gas turbine cycle power conversion system was developed in the early 1990s [1]. Research and development activities on next generation nuclear reactors are ongoing in many countries with the aim of realizing efficient and economic power generation. In this regard, helium gas turbines have been extensively investigated for reactor applications, particularly with respect to achieving high efficiency in electricity generation based on a closed Brayton cycle as a replacement for the conventional steam Rankine cycle. The Pebble Bed Modular Reactor (PBMR), the Gas Turbine Modular High Ttemperature Reactor (GT-MHR), and the Gas Turbine High Temperature Reactor of 300 MWe nominal capacity (GTHTR 300) are representative programs employing the helium gas turbine cycle.

A key virtue of the gas turbine is very high power output relative to its size. Accordingly, gas turbines have been used for jet propulsion in aircrafts and power generation in power plants for many years, and considerable experience related to open cycle air-breathing gas turbines has been accumulated. Existing technologies applied to air-breathing gas turbines can be basically employed for closed cycle helium turbomachinery. Helium gas has been regarded as a proper choice for the HTGR gas turbine due to its radioactive stability and high thermal capacity. Although the helium gas turbine design follows the existing design practice for combustion gas turbines, there are obvious differences because of the physical properties of helium and the pressure condition in the nuclear application. The unique characteristics of the helium gas turbine are a shorter blade height and a larger number of stages compared with the air gas turbine. The shorter blade height leads to an increase in the leakage flow through the blade tip clearance, resulting in a higher loss in the efficiency. A longer flow passage from a larger number of stages causes end-wall boundary layer growth and secondary flow, also resulting in a higher loss in the efficiency. As the hub-to-tip ratios of the helium compressor are high, around 0.9 throughout all the stages, consideration of secondary flow loss in the blading design is crucial for attaining better efficiency and a higher stall margin. Also, advanced blading techniques are needed to eliminate flow separation and a blade over-camber is required to compensate for flow distortion near the end-wall. The seal mechanism for helium is also much more complex than that for air or steam.

However, the helium gas turbine also offers important advantages, including a lower Mach number and a higher Reynolds number than the air-breathing gas turbine. As the flow in a compressor decelerates, the losses due to the tip clearance and secondary flow through the compressor can be more substantial than in the turbine. While the estimation

of the losses in the air compressors is sufficiently accurate because of extensive related design and operating experiences, very limited experiences have been obtained with axial helium gas compressors.

The present study focuses on helium gas turbines from a thermodynamic point of view. Detailed discussion of the stress and vibration analysis or the design of magnetic bearings is beyond the scope of this report. This report provides a review of operational experiences of helium turbomachinery and describes the design and availability of the HTGR helium Brayton cycle. We have also developed a new throughflow analysis code capable of estimating the design-point performance of the helium gas turbine. The aerodynamic performance of GTHTR300 gas turbines has been investigated using the throughflow calculation.

2. BACKGROUND

Although many technical experiences have been accumulated since the operation of the Dragon, AVR, Peach Bottom, THTR, and FSV reactors, the crucial design aspects of a helium Brayton cycle have not been assessed or verified. Experience with design and operation of closed cycle helium gas turbines have been limited. There are earlier experiences gained from two test facilities in Germany [2] and a recent test program to simulate the performance of a 1/3-scale multi-stage helium compressor of GTHTR300 in Japan [3].

2.1 Earlier Helium Brayton Cycle Experience

All earlier HTGRs installed steam cycles, because they were a mature technology at that time while helium gas turbine technology was not well matured. Use of the steam turbine cycles led to an indirect cycle with a steam generator. Use of the steam turbine cycles causes several problems: an increase in capital cost and possibility of water ingress, high maintenance requirements of the steam generator tubes, and use of a gas circulator. Recent HTGR design proposes implementation of a helium gas turbine cycle rather than a steam turbine cycle. This change leads to an increase in helium temperature, the direct cycle, and implementation of a modular concept with a compact, factory-assembled helium cycle. The direct cycle enables elimination of the steam generator as well as the circulator. The size of the blades in a helium turbine is around 0.1 m whereas the blades are larger than 1 m in the steam turbine. As a result, the HTGR is economically competitive with large-scaled water reactors even though the power level of the former is much lower than that of the latter. Therefore, the technology of the helium turbine cycle is essential in development of the HTGR.

The first and largest helium turbine to date was constructed in Germany in 1968. It was rated at 50 MWe at 750°C. Note that the largest helium turbine under design has an output of 400 MWe as GT-MHR. It was experimentally tested in a high-temperature, helium cooled nuclear reactor heat source generated by a fossil-fired heater with 53.5 MW for electricity generation (the HHT project) in 1968. The operating pressure for tests was up to around 1 MPa. The HHT project involved two experimental facilities. The first was an Oberhausen II helium turbine cogeneration plant operated from 1974 to 1988 by the German utility EVO (Energie Versorgung Oberhausen AG). The second facility was a high-temperature test plant (HHV) built in 1981. The main issues solved through these tests were material performance of the high temperature blades and disks and dynamic issues of rotor and magnetic bearings.

The EVO was a milestone test facility that played an important role in the development of current HTGRs. For the turbomachinery, a two-shaft arrangement with an interconnected gear was selected. The high-pressure (HP) turbine, which has a rotational speed of 5,500 rpm, drives the low-pressure (LP) compressor and high-pressure (HP) compressor on the first shaft. The low-pressure (LP) turbine is directly connected to the generator with a synchronous rotational speed of 3,000 rpm. The mass flow rate of helium is 84.8 kg/s. A photograph of the HP turbine rotor is shown in Fig. 1. The HP turbine and the LP turbine have 7 stages and 11 stages, respectively. The HP compressor and the LP compressor have 15 stages and 10 stages, respectively, both with 100% reaction. The EVO facility was operated for approximately 24,000 hours. However, the maximum electricity power output of EVO was 30.5 MWe, which is much less than the design power considered for an HTGR with a helium Brayton cycle.

The HHV has an electrically-driven turbomachinery consisting of a 2-stage turbine and an 8-stage compressor on a single-shaft arrangement with a synchronous rotational speed of 3,000 rpm. Fig. 2 shows a picture of the HHV turbine. The compressor requires 90 MW power, the turbine power produces about 46 MW, and the electric motor supplies 45 MW. The mass flow rate is about 200 kg/s. During the initial operation, oil ingress and excessive helium leakage occurred. After the problems were corrected, the HHV test plant was successfully operated for about 1,100 hours, and the measured results showed that the helium gas turbine had a higher efficiency than the design value. They found that creep and fatigue crack growth at high temperature with impurities such as carbon in the helium coolant comprises the main mechanism limiting the lifetime of the turbine blades and disks. Also, it was estimated that the lifetimes of uncooled turbine components are around 50,000-60,000 hours and that the maximum temperature with uncooled metallic blades and disks is 850°C.

2.2 Recent Helium Turbomachinery Tests

In 2003, a scaled-down test model of the first 4 stages of the GTHTR300 compressor was designed and fabricated in the Japanese test program to test the aerodynamic performance and verify the design and evaluation methods [3]. Three major tests were planned: a compressor aerodynamic

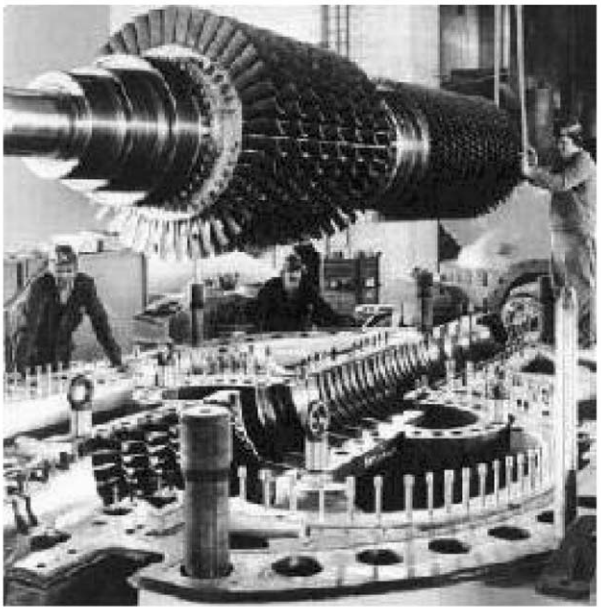

Fig. 1. High-pressure Turbine Rotor from EVO in Germany

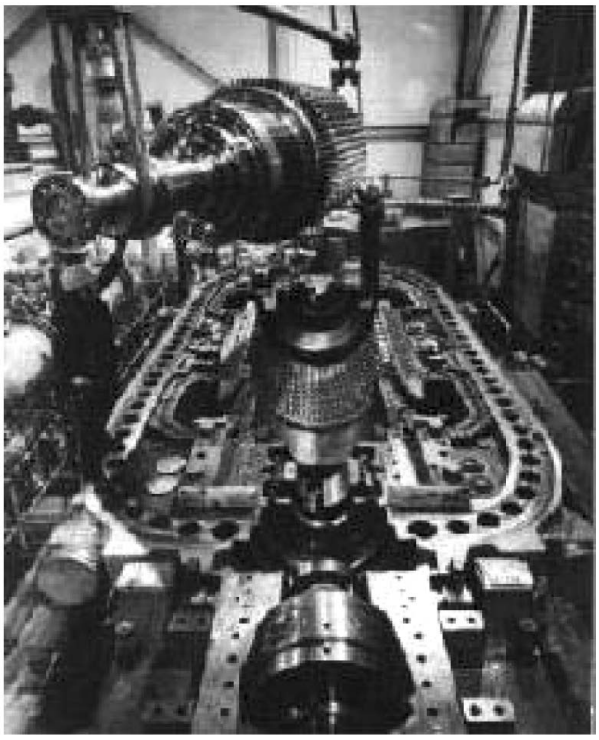

Fig. 2. Rotor from HHV in Germany

performance test, a magnetic bearing development test, and a gas-turbine system operation and control test. Fig. 3

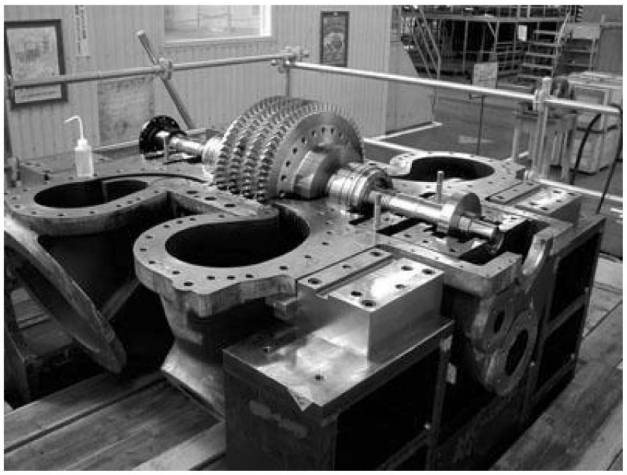

Fig. 3. 1/3-scale Helium Compressor Model in Japan

Table 1. Major Design Parameters of the 1/3-Scale Compressor Model

Mass flow rate (kg/s)	12.2
Inlet temperature (°C)	30
Inlet pressure (MPa)	0.883
Pressure ratio	1.156
Hub diameter (mm)	500
Tip diameter (1st stage, mm)	568
Hub-to-tip ratio (1st stage)	0.88
Number of stages	4
Rotational speed (rpm)	10800
Circumferential speed of rotor blade (m/s)	321
Number of rotor/stator blades (1st stage)	72/94
Rotor/stator blade chord length (1st stage, mm)	28.6/35
Rotor/stator blade height (1st stage, mm)	34/33.7

shows a picture of the test model. A 1/3-scale, 4-stage mockup was selected to reproduce the stage interaction, the boundary layer growth, and the repeating stage flow observed in the prototypic compressor. The test compressor is driven by an electric motor of 3.65 MW with 10,800 rpm. The operating fluid is helium gas whose pressure is up to around 1 MPa. Its rotational speed is three times higher than that of the prototype so as to match the circumferential speed and the Mach number. It includes magnetic bearings

to support the turbo-compressor rotor and the generator rotor instead of oil bearings in order to eliminate the possibility of oil ingress into the reactor. Major design parameters are presented in Table 1.

The magnetic bearing development test is implemented to develop the technology of the magnetic bearing supported rotor system. It consists of a 1/3-scale turbo-compressor and generator rotor models. The rotor models were designed so that both the critical speeds and vibration modes may be matched to those of the prototypic rotors. Its test matrix includes testing of magnetic bearing performance, unbalance response, stability, and auxiliary bearing reliability.

The test facility for the gas-turbine system operation and control test consists of a turbine, a compressor, a dynamometer, a recuperator, a pre-cooler, and a heater. The turbine and the compressor have a single stage and four stages, respectively, with a nominal pressure ratio of 1.156. The design pressure, design temperature, rated flow rate are 1.09 MPa, 650°C and 12.2 kg/s, respectively. Transient tests are planned: start-up, shutdown, load change, loss of load, and emergency shutdown.

3. HTGR HELIUM GAS TURBINES

For closed cycle gas turbines, helium is considered a promising working fluid because it has many favorable aspects for HTGR application. Helium is an inert gas that is non-corrosive and does not become radioactive. The cycle efficiency has a theoretical advantage owing to the high specific heat ratio of helium. The choice of working fluid significantly influences not only the cycle efficiency but also the system compactness. Additionally, the heat exchanger design also is advantageous because the thermal conductivity and heat transfer coefficient for helium are higher than those for air. On the other hand, helium leakage could easily occur due to its low molecular weight and thus reliable sealing of the system is imperative. As outlined above, HTGR helium gas turbines differ from other gas turbines using air or combustion gases.

3.1 General Features of HTGR Helium Gas Turbines

The fluid properties of helium strongly influence the size, geometries, and performance of gas turbine. High pressure operation is needed to achieve a compact power conversion system in the HTGR. The helium gas turbines have high hub-to-tip ratios throughout the machine because the rotational speed is restricted to the synchronous speed when the turbomachines are directly connected to the generator. A comparison of the design parameters between air-breathing compressors and HTGR helium compressors is given in Table 2 [4-6]. Although helium compressors are operated at a low pressure ratio, the specific heat and specific heat ratio are high, and consequently the compressor needs a large number of stages to achieve the required pressure ratio. These design features unfavorably affect the aerodynamic performance. A low blade aspect ratio tends to increase the secondary flow and tip leakage flow, and many stages tend to increase the end-wall boundary layer growth and secondary flow. On the other hand, it is possible to provide higher circumferential speeds without approaching the sonic range due to the high sonic velocity of helium. In addition, shock loss also can be neglected in the design-point operation.

3.2 PBMR Turbomachinery

The design of the power conversion unit (PCU) of the PBMR has been modified several times. In the original design, the PBMR power conversion unit has a 3-shaft vertical arrangement including a LP turbo-unit, HP turbo-unit, and a power turbine with a generator, as shown in Fig. 4 [7]. Each rotor is housed in each vessel. This necessitates smaller capacity of the axial magnetic bearing and its associated catcher bearing, small temperature and pressure variations, and shorter rotor length due to multi-rotors. The issues raised in the vertical multi-shaft configuration are cost problems, an overspeed problem in the case of load rejection, and pressure seal and reliability in the structural design because of complicated flow pass.

As a result, the turbomachinery configuration was modified to a single-shaft horizontal arrangement that has a rotational speed of 6,000 rpm with a reduction gear to 3,000 rpm for the generator. Fig. 5 presents a schematic of the latest PBMR PCU [8].

3.3 GTHTR300 Turbomachinery

The gas turbine cycle of the GTHTR300 is designed to generate 275 MWe power for 600 MW reactor thermal

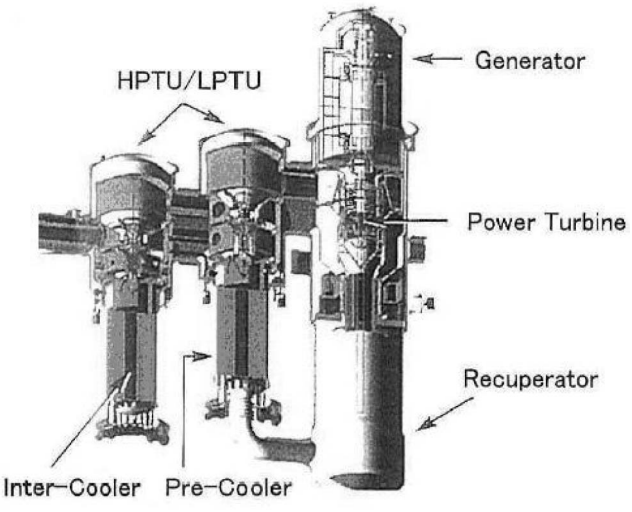

Fig. 4. Plant Layout of Previous PBMR Design

Table 2. Comparison of Design Parameters Between Air Compressors and HTGR Helium Compressors

Unit	Air-Breathing Compressors			Helium Compressors		
	C135	C141	NACA	GTHTR300	GT-MHR	
					LP	HP
Number of stages	2	4	8	20	14	19
Design pressure ratio	1.88	2.95	10.26	2.00	1.70	1.70
Inlet hub-to-tip ratio	0.38	0.69	0.48	0.88	0.87	0.90
Exit hub-to-tip ratio	0.57	0.81	0.90	0.91	0.88	0.90
Mass flow/unit annulus area ($kg/s.m^2$)	207	189	189	447	591	1141
Blade tip speed (1^{st}, m/s)	423.0	362.0	356.0	321.0	301.7	245.8

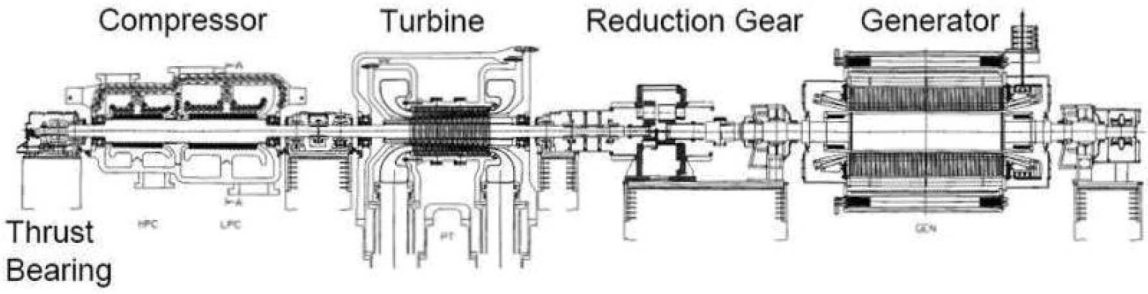

Fig. 5. Configuration of the Latest PBMR PCU

power with a mass flow rate of about 442 kg/s [5]. A single-shaft horizontal arrangement is adopted, as shown in Fig. 6. The 20-stage compressor requires 251 MW with a pressure ratio of 2.0. The turbine is a 6-stage unit with a pressure ratio of 1.87, which produces 530 MW. The electric generator converts 279 MW shaft power input into 275 MW electric output at 98.5% efficiency. The rated rotational speed of the rotor system is 3,600 rpm. The low cycle pressure ratio simplifies the gas turbine mechanical design with optimum cycle without an intercooler. This configuration minimizes research and development work, and is very effective in terms of protecting against overspeed of the rotor in the case of load rejection. Its drawback is the requirement of a larger building area for the horizontal turbine vessel and associated rotor space.

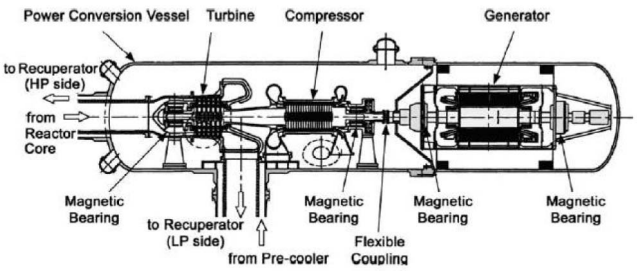

Fig. 6. Cross-section of the GTHTR300 Turbomachine

3.4 GT-MHR Turbomachinery

As shown in Fig. 7, the GT-MHR turbomachine is a vertical single shaft configuration at a synchronous rotational speed of 3,000 rpm [6]. The turbo-compressor rotor consists of a 24-stage HP compressor, a 16-stage LP compressor, and a 7-stage turbine. The turbomachine and generator rotors are rigidly connected by a coupling that provides transmission of torque between these rotors. The compre-

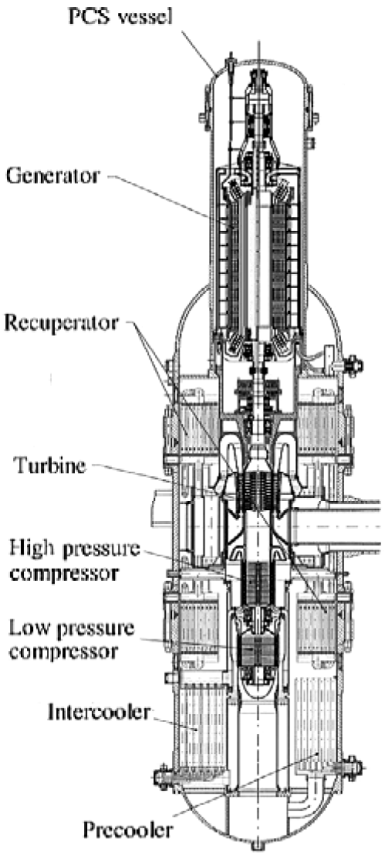

Fig. 7. Plant Layout of the GT-MHR

ssors require 276 MW, the turbine power produces about 561 MW, and the power generation is 285 MW.

All the power conversion components are housed in a single vessel, making it both extremely compact and economical. The issues raised in the vertical single-shaft configuration are a shaft vibration problem, the large capacity requirement of the axial magnetic bearing and its associated catcher bearing, and large temperature and pressure variations.

4. ESTIMATION OF PERFORMANCE

Axisymmetric throughflow calculations are an essential part of the conceptual design and analysis of gas turbines. In this paper, the flow field in the gas turbine is analyzed according to the streamline curvature throughflow method presented by J.D. Denton [9] with applicability to a wide range of geometries. The total enthalpy increases in the compressor and decreases in the turbine by deflection of the flow in passing the rotors, as noted from the Euler turbomachine equation. Empirical loss models for the compressor and turbine are also required to reflect viscous effects, which play an important part in evaluating the performance of a gas turbine.

4.1 Streamline Curvature Method

From the description given by J.D. Denton, the total acceleration of a fluid particle a_q in the direction of the unit vector q can be given as follows:

$$a_q = V_m \frac{\partial V_m}{\partial m}\cos\alpha_q + \frac{V_m^{\,2}}{r_c}\sin\alpha_q - \frac{V_\theta^{\,2}}{r}\sin(\phi+\alpha_q) \qquad (1)$$

The momentum equation applied in the stream surface in the direction of q is then

$$-\frac{1}{\rho}\frac{\partial p}{\partial q} = T\frac{\partial s}{\partial q} - \frac{\partial h}{\partial q} = a_q \qquad (2)$$

Therefore, the equation for the gradient in the direction of the quasi-orthogonal in the meridional surfaces is

$$\frac{1}{2}\frac{d}{dq}V_m^{\,2} = \frac{dh_0}{dq} - T\frac{ds}{dq} - \frac{1}{2r^2}\frac{d\left(r^2V_\theta^2\right)}{dq} + \frac{V_m^2}{r_c}\sin\alpha_q + V_m\frac{dV_m}{dm}\cos\alpha_q \qquad (3)$$

This equation is called the radial equilibrium equation and is the basis of all throughflow calculation methods. The first three terms on the right hand side of equation (3) will be referred to as radial equilibrium terms and the last two terms as streamline curvature terms.

Equation (3) must be solved in conjunction with the continuity equation as follows:

$$\dot{m} = \int_{r_{hub}}^{r_{tip}} 2\pi r b \rho V_m \sin\alpha \; dq \qquad (4)$$

where b is a measure of blockage and would be unity in an ideal case.

4.2 Euler Turbomachine Equation

4.2.1 Axial-flow Compressor

A typical stage of an axial-flow compressor is shown in Fig. 8. Assuming the flow of a streamline that enters the rotor at one radius and leaves at another radius with another

velocity, the change in angular momentum in passing the rotor produces an enthalpy increase [10]. The process through the rotor and stator can be assumed to be adiabatic, and there is an increase in stagnation pressure only within the rotor and a decrease in the stagnation pressure in the stator due to fluid friction. By applying the steady flow energy equation to the rotor, the power input is given by

$$P = \dot{m} C_p \left(T_{02} - T_{01} \right) \tag{5}$$

There is no work input in the stator and thus the stagnation temperatures of positions 2 and 3 are the same.

Fig. 9 shows the velocity vectors and associated velocity diagram for a typical stage. The fluid approaches the inlet of the rotor with a velocity V_1 at an angle α_1 and the relative velocity W_1 at β_1 results from the blade speed U. The fluid is deflected through the rotor, and the fluid leaves the rotor with a relative velocity W_2 at β_2. Considering the blade speed, the velocity V_2 is given at an angle α_2. The tangential velocities $V_{\theta 1}$ and $V_{\theta 2}$, are found from the meridional velocity V_m and the flow angles, and these tangential velocities can produce a change in enthalpy through work transfer. An increase of total enthalpy is obtained from the Euler turbomachine equation along the streamlines as follows:

$$\Delta h_0 = \omega (r_2 V_{\theta 2} - r_1 V_{\theta 1}) \tag{6}$$

Therefore, the power input to the stage can be expressed as follows:

$$P = \dot{m} \omega (r_2 V_{\theta 2} - r_1 V_{\theta 1}) \tag{7}$$

This input energy is absorbed usefully in raising the pressure of the fluid, and the pressure rise is dependent on the efficiency of the compression process. The stage pressure ratio is given by

$$\frac{p_{03}}{p_{01}} = \left[1 + \frac{\eta_{S,C} \Delta h_0}{h_{01}} \right]^{\gamma/(\gamma-1)} \tag{8}$$

where $\eta_{S,C}$ is the isentropic efficiency of compressor.

4.2.2 Axial-flow Turbine

Fig. 10 shows a typical axial-flow turbine stage. Similarly, the flow of a streamline enters the rotor at one radius and leaves at another radius with another velocity. The change in angular momentum in passing the rotor comes from the enthalpy decrease [10]. The process through the rotor and stator is adiabatic, and the stagnation pressure decreases in the stator due to fluid friction. There is a decrease in stagnation pressure only within the rotor. There is no work in the stator and hence the stagnation temperatures of positions 1 and 2 are the same. By applying the steady flow energy equation to the rotor, the power input is given by

$$P = \dot{m} C_p \left(T_{03} - T_{02} \right) \tag{9}$$

The velocity vectors and associated velocity diagram for

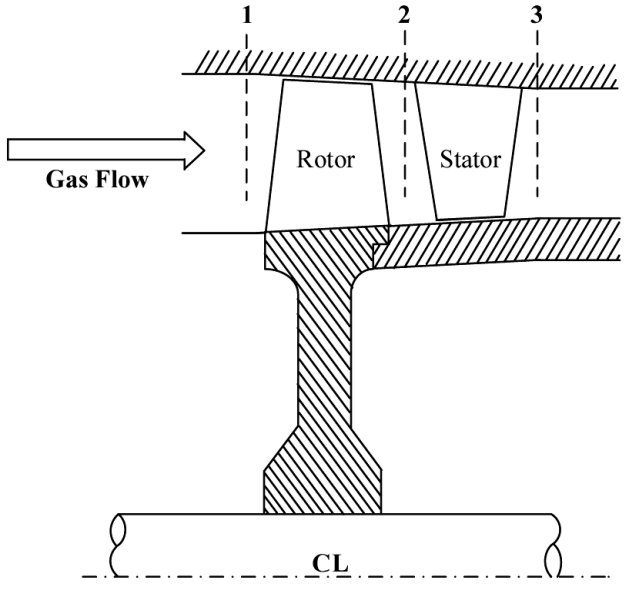

Fig. 8. Typical Axial-flow Compressor Stage

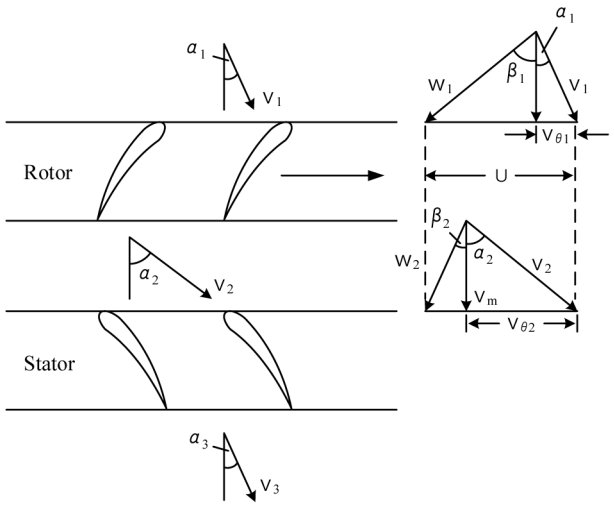

Fig. 9. Velocity Triangles for a Compressor Stage

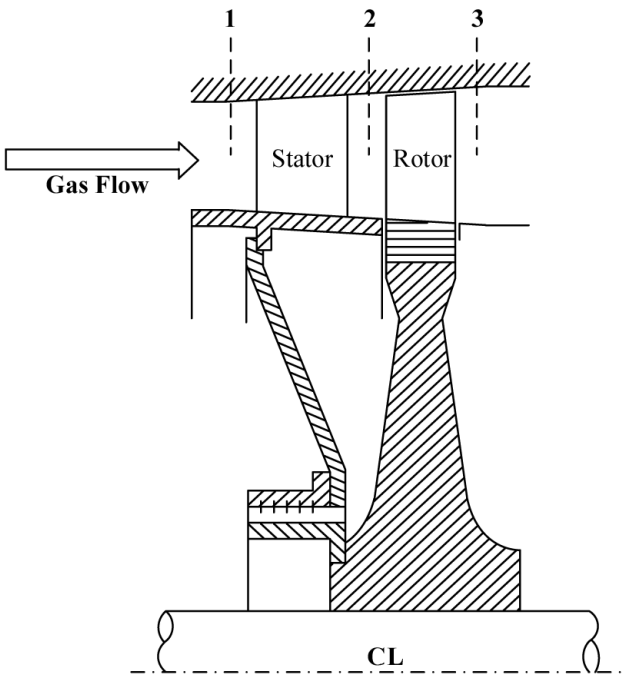

Fig. 10. Typical Axial-flow Turbine Stage

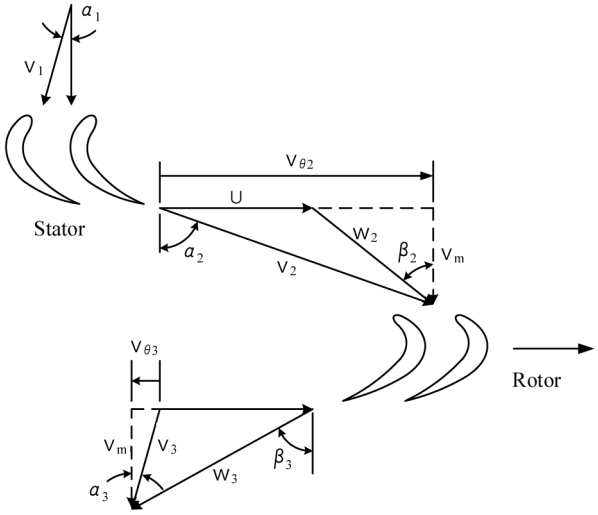

Fig. 11. Velocity Triangles for a Turbine Stage

a typical stage are shown in Fig. 11. The fluid approaches the inlet of the stator with a velocity V_1 at an angle α_1. The fluid is deflected through the stator, and the fluid leaves the rotor with a velocity V_2 at α_2 resulting from the blade speed U and the relative velocity W_2 at β_2. The fluid is deflected through the rotor and leaves the rotor with a relative velocity W_3 at β_3, and the velocity V_3 is given at an angle α_3. The tangential velocities $V_{\theta 2}$ and $V_{\theta 3}$ are found from the meridional velocity V_m and the flow angles, and these tangential velocities can produce work through the change in enthalpy.

A decrease of total enthalpy is obtained from the Euler turbomachine equation along the streamlines.

$$\Delta h_0 = \omega(r_2 V_{\theta 2} - r_3 V_{\theta 3}) \tag{10}$$

The power input to the stage can be expressed as follows:

$$P = \dot{m}\omega(r_2 V_{\theta 2} - r_3 V_{\theta 3}) \tag{11}$$

This input energy is absorbed usefully in raising the pressure of the fluid, and the pressure rise is dependent on the efficiency of the compression process. The stagnation pressure ratio of the stage can be found from

$$\Delta T_{0S} = \eta_{S,T} T_{01}\left[1 - \left(\frac{1}{p_{01}/p_{03}}\right)^{(\gamma-1)/\gamma}\right] \tag{12}$$

where $\eta_{S,T}$ is the isentropic efficiency of turbine.

4.3 Losses and Performance Estimation

The efficiency is dependent on the total drag coefficient for each of the blade rows and the flow path, and there are four kinds of primary loss sources. First, the profile loss is caused by the flow around the blade boundary layers and the wake of the trailing edge. The annulus loss is associated with the end-wall boundary layers, and the secondary flow loss is due to the cascade and trailing vortices. Lastly, the tip clearance loss is due to the leakage through the tip clearances. In the design of a HTGR helium gas turbine, the shock loss is not considered because helium gas has a very high sonic velocity and the compressor operates only in the low subsonic region.

The analysis below is applied to the loss prediction at the design-point. The loss models are widely accepted and recommended by GE and Concept-NREC and can be found in references [11] through [16].

5. RESULTS AND DISCUSSION

The GTHTR300 compressor and turbine design of JAEA have been selected to verify the code results, because the details of the design specifications and geometry are available [5]. Tables 3 and 4 summarize the design parameters. The compressor has a constant inner wall diameter and the turbine has a constant mean diameter design. The

Table 3. GTHTR300 Compressor Specifications of KAIST Simulation

Mass flow rate (kg/s)	449.7
Inlet temperature (°C)	28
Inlet pressure (MPa)	3.52
Pressure ratio	2.00
Hub diameter (mm)	1500
Tip diameter ($1^{st}/20^{th}$ stage, mm)	1704/1645
Hub-to-tip ratio ($1^{st}/20^{th}$ stage, mm)	0.88/0.91
Number of stages	20
Rotational speed (rpm)	3600
Number of rotor/stator blades (1^{st} stage)	72/94
Rotor/stator blade chord length (1^{st} stage, mm)	78/60
Rotor/stator blade height (1^{st} stage, mm)	102/101
Polytropic efficiency (%)	90.5

Table 4. GTHTR300 Turbine Specifications of KAIST Simulation

Mass flow rate (kg/s)	441.8
Inlet temperature (°C)	850
Inlet pressure (MPa)	6.88
Pressure ratio	1.87
Hub diameter ($1^{st}/6^{th}$ stage, mm)	1844/1750
Tip diameter ($1^{st}/6^{th}$ stage, mm)	2156/2250
Hub-to-tip ratio ($1^{st}/6^{th}$ stage, mm)	0.855/0.778
Number of stages	6
Rotational speed (rpm)	3600
Number of stator/rotor blades (1^{st} stage)	82/80
Rotor/stator blade chord length (1^{st} stage, mm)	78/60
Stator/rotor blade height (1^{st} stage, mm)	150/156
Polytropic efficiency (%)	92.8

gas turbine has unique design features such as short blade height and a large number of stages, as stated above.

The throughflow calculation was performed in order to predict the flow velocity inside the gas turbines and evaluate the performance based on the detailed geometry of the compressor and turbine. The loss models, which are adopted here, work reasonably in the case of helium gas turbines. A performance comparison of JAEA and KAIST at the design-point show that they are in good agreement: the errors are within $\pm 1.5\%$ in terms of pressure ratio, temperature ratio, polytropic efficiency, and shaft work.

6. CONCLUDING REMARKS

Remarkable advances in helium turbomachinery technology have led to the design and fabrication of large-scale helium turbomachines in HTGR applications. HTGR helium gas turbines have low pressure ratio, high operating pressure, short blade height, and a large number of blades compared to air gas turbines. The single-shaft system is considered a feasible configuration and a horizontal arrangement is preferred over the vertical case.

The GTHTR300 gas turbines are simulated using the throughflow analysis code developed by KAIST, and consequently the design-point performance of the gas turbine is well predicted compared with the JAEA data.

REFERENCES

[1] "Current Status and Future Development of Modular High Temperature Gas Cooled Reactor Technology," IAEA-TECDOC-1198, 2001.
[2] "Summary Report on Technical Experiences from High-Temperature Helium Turbomachinery Testing in Germany," IAEA-TECDOC-899, pp. 177-248, 1995.
[3] S. Takada, T. Takizuka, et al., "The 1/3-scale Aerodynamics Performance Test of Helium Compressor for GTHTR300 Turbo Machine of JAERI (STEP1)," Proceeding of ICONE11, Tokyo, Japan, April 20-23, 2003.
[4] A.R. Howell and W.J. Calvert, "A New Stage Stacking Technique for Axial-Flow Compressor Performance Prediction," Journal of Engineering for Power, Transactions of the ASME, Vol. 100, pp. 698-703, 1978.
[5] T. Takizuka, S. Takata, et al., "R&D on the Power Conversion System for Gas Turbine High Temperature Reactors," Nuclear Engineering and Design, North-Holland Publishing Company, pp.329-346, 2004.
[6] "Summary Report on Technical Experiences from High-Temperature Helium Turbomachinery Testing in Germany," IAEA-TECDOC-899, pp. 177-248, 1995.
[7] "PBMR Project Status and the Way Ahead," 2nd International Topical Meeting on High Temperature Reactor Technology, Beijing, China, September 22-24, 2004.
[8] Regis A. Matzie, "Pebble Bed Modular Reactor (PBMR) Project Update," Presentation of Westinghouse Electric Company, June 16, 2004.
[9] J.D. Denton, "Throughflow Calculation for Transonic Axial Flow Turbines", Journal of Engineering for Power, Transactions of the ASME, Vol. 100, pp. 212-218, 1978.
[10] H.I.H. Saravanamuttoo, G.F.C. Rogers and H. Cohen, "Gas Turbine Theory," Prentice Hall, 2001.
[11] C.C. Koch and L.H. Smith, "Loss Sources and

Magnitudes in Axial-flow Compressors," Journal of Engineering for Power, Transactions of the ASME, pp. 411-424 (1976).
[12] B. Lakshiminarayana and J.H. Horlock, "Review: Secondary Flows and Losses in Cascades and Axial-flow Turbomachines," International Journal of Mechanical Sciences, Pergamon Press Ltd, Vol. 5, pp.287-307, 1963.
[13] B. Lakshminarayana, "Methods of Predicting the Tip Clearance Effects in Axial Flow Turbomachinery," Journal of Basic Engineering, Transactions of the ASME, pp. 467-482, 1970.
[14] O.E. Balje and R.L. Binsley, "Axial Turbine Performance Evaluation. Part A – Loss-Geometry Relationship," Journal of Engineering for Power, Transactions of the ASME, pp. 341-348, 1968.
[15] S.C. Kacker and U. Okapuu, "A Mean Line Prediction Method for Axial Flow Turbine Efficiency," Journal of Engineering for Power, Transactions of the ASME, pp. 111-119, 1982.
[16] J. Dunham and P.M. Came, "Improvements to the Ainley-Mathieson Method of Turbine Performance Prediction," Journal of Engineering for Power, Transactions of the ASME, pp. 252-256, 1970.